Published August 6, 2012

A role for apoptosis-inducing factor in T cell development

Hridesh Banerjee,[1] Abhishek Das,[1] Smita Srivastava,[1] Hamid R. Mattoo,[1] Krishnamurthy Thyagarajan,[1] Jasneet Kaur Khalsa,[1] Shalini Tanwar,[1] Deepika Sharma Das,[1] Subeer S. Majumdar,[1] Anna George,[1] Vineeta Bal,[1] Jeannine M. Durdik,[2] and Satyajit Rath[1]

[1]National Institute of Immunology, New Delhi 110067, India
[2]Department of Biological Sciences, University of Arkansas, Fayetteville, AR 72701

Apoptosis-inducing factor (Aif) is a mitochondrial flavoprotein that regulates cell metabolism and survival in many tissues. We report that *aif*-hypomorphic harlequin (Hq) mice show thymic hypocellularity and a cell-autonomous thymocyte developmental block associated with apoptosis at the β-selection stage, independent of T cell receptor β recombination. No abnormalities are observed in the B cell lineage. Transgenes encoding wild-type or DNA-binding–deficient mutant Aif rectify the thymic defect, but a transgene encoding oxidoreductase activity–deficient mutant Aif does not. The Hq thymic block is reversed in vivo by antioxidant treatment, and Hq T but not B lineage cells show enhanced oxidative stress. Thus, Aif, a ubiquitous protein, serves a lineage-specific nonredundant antiapoptotic role in the T cell lineage by regulating reactive oxygen species during thymic β-selection.

CORRESPONDENCE
Satyajit Rath:
satyajit@nii.res.in

Abbreviations used: Aif, apoptosis-inducing factor; DCFDA, 2′-7′-dichlorofluorescein diacetate; DN, double-negative; DP, double-positive; EdU, 5-ethynyl-2′-deoxyuridine; Hq, harlequin; mBCl, monochlorobimane; NID, neglect-induced death; ROS, reactive oxygen species; SOD, superoxide dismutase; SP, single-positive; tg, transgenic.

Apoptosis-inducing factor (Aif) is a ubiquitously expressed flavoprotein with NADH oxidase activity located in the mitochondrial intermembrane space (Candé et al., 2002). In mitochondria, Aif appears to be important in regulating oxidative phosphorylation and reactive oxygen species (ROS) levels to mediate antiapoptotic functions in vivo, as shown by studies with tissue-specific Aif deficiency (Joza et al., 2005; Pospisilik et al., 2007; Ishimura et al., 2008) with the harlequin (Hq) strain of mice, which have a proviral insertion in the upstream regulatory region of the *aif* gene leading to Aif hypomorphism (Klein et al., 2002), and with the identification of a human Aif-associated myopathy (Ghezzi et al., 2010). However, when released from mitochondria upon activation of intrinsic death pathways, Aif can cause nuclear DNA degradation, a proapoptotic function possibly critical for embryonic development (Joza et al., 2001). Curiously, in many of these examples, Aif deficiency appears to have tissue- and cell lineage–specific effects despite the ubiquitous nature of Aif expression. Although there is both indirect (Ferri et al., 2000; Bidère and Senik, 2001) and direct (Srivastava et al., 2007) evidence that Aif participates in death pathways in peripheral T cells, it is not yet clear if there are in vivo consequences of such roles in T cell development.

T lineage cells undergo extensive proliferation and death at multiple points during intrathymic development, starting from the early $CD4^{-}CD8^{-}$ (double-negative; DN) stages. DN cells with nonproductively rearranged TCR-β loci undergo neglect-induced death (NID) via mitochondrial pathways (Strasser and Bouillet, 2003). Cells that successfully express TCR-β enter a pre-TCR–induced program of

H. Banerjee, A. Das, and S. Srivastava contributed equally to this paper.
A. George, V. Bal, J.M. Durdik, and S. Rath contributed equally to this paper.
H. Banerjee's present address is Laboratory of Molecular Biology and Immunology, National Institute of Aging, Baltimore, MD 21224.
A. Das's present address is Immune Disease Institute, Children's Hospital Boston, Boston, MA 02115.
S. Srivastava's present address is Division of Infectious Diseases, Dept. of Medicine, New York University School of Medicine, New York, NY 10016.
H.R. Mattoo's present address is MGH Cancer Center, Charlestown, MA 02129.
K. Thyagarajan's present address is Dept. of Surgery, Medical University of South Carolina, Charleston, SC 29425.

The Rockefeller University Press $30.00
J. Exp. Med. 2012 Vol. 209 No. 9 1641-1653
www.jem.org/cgi/doi/10.1084/jem.20110306

Published August 6, 2012

proliferation and differentiation, leading to their entry into the $CD44^{-}CD25^{-}$ (DN4) and thence into the $CD4^{+}CD8^{+}$ (double-positive; DP) stage via the process of β-selection (Hoffman et al., 1996). Survival during β-selection depends on several factors, ranging from IL-7–IL-7R interactions (Trigueros et al., 2003) and adenosine deaminase–mediated ATP clearance (Van De Wiele et al., 2002; Thompson et al., 2003) to the availability of the small GTPase Rho (Cleverley et al., 1999; Costello et al., 2000) and the death protein PD-1 (Nishimura et al., 2000). DP cells productively rearranging their TCR-α loci but failing positive selection die, possibly by yet another form of NID controlled by the nuclear retinoic acid–related orphan receptor γ (Sun et al., 2000). Interestingly, the broad-spectrum caspase inhibitor protein baculovirus p35 has been reported to leave thymic selection unaffected, although a contrary finding has been reported as well (Izquierdo et al., 1999; Doerfler et al., 2000). It is thus possible that multiple interacting death pathways are involved during early thymocyte development and that some of these may be caspase independent.

On this background, we have investigated the Hq mouse strain, which shows a 5–10-fold reduction in Aif expression levels (Klein et al., 2002), for a potential T cell lineage–specific developmental role for Aif, and we show that Aif expression in T lineage cells and its function in regulating ROS levels is critical for their successful transition through β-selection.

RESULTS

Aif hypomorphic Hq mice show a naive T cell deficit in the periphery

There was a substantial reduction in the frequency of both CD4 and CD8 T cells in the spleen and lymph nodes of 8–12-wk-old Hq mice (Fig. 1 A). Although the absolute total cell numbers in spleen and LN were not consistently different between WT and Hq mice, frequencies (Fig. 1 B) and absolute numbers of CD4 and CD8 cells were significantly low (Fig. 1, C and D). This was specific to the T cell compartment because the numbers of either macrophages or B cells showed little or no difference (Fig. 1 E). This T cell–specific attrition was more prominent in the phenotypically naive $CD44^{low}$ population as compared with the $CD44^{high}$ effector/memory population (Fig. 1, F and G).

Hq mice have a T lineage cell-autonomous thymic developmental blockade

We therefore explored the possibility that Aif deficiency had an effect on T lineage cell development in the thymus. In 8–12-wk-old mice, the Hq thymus was significantly hypocellular compared with the WT thymus, and the difference was most prominent in the $CD4^{-}CD8^{+}$ single-positive (SP;CD8SP), $CD4^{+}CD8^{-}$ CD4SP, and DP cells but was less marked in the DN cells (Fig. 2, A and B). However, γ/δ T cell numbers were not reduced in the Hq thymus (γ/δ cells/thymus [mean + SE]: $0.75 \times 10^{6} + 0.35$ [WT], $1.7 \times 10^{6} + 0.53$ [Hq]; $P > 0.1$).

We next tested whether a relative lack of Aif specifically in T lineage cells and/or in thymic stromal cells was required for

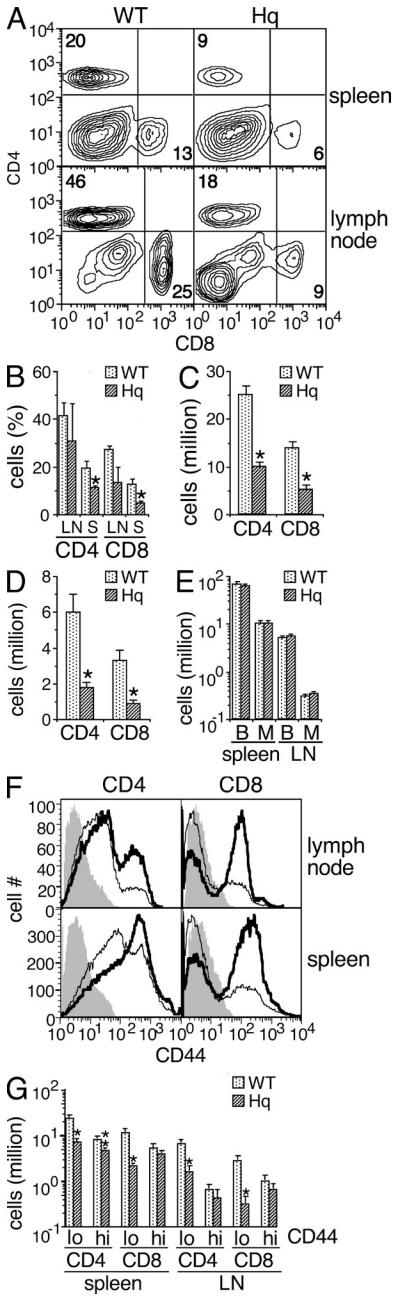

Figure 1. Deficit of naive T cells in the peripheral lymphoid organs of Aif-hypomorphic Hq mice. (A) Representative two-color analyses of splenic and lymph node cells from 8–12-wk-old WT and Hq mice stained for CD4 and CD8, showing frequencies of cells in quadrants. (B–D) Frequencies (B) and absolute numbers of CD4 and CD8 cells in the spleen (C) and inguinal lymph node (D) of WT and Hq mice. *, $P < 0.01$. (E) Absolute numbers of $B220^{+}$ B cells (B) and $CD11b^{+}$ macrophages (M) in the spleen (S) and inguinal lymph node (LN) of WT and Hq mice. (F) Representative analysis of CD44 levels on gated CD4 or CD8 cells from spleen or lymph nodes of WT (thin lines) or Hq (thick lines) mice. Filled histograms represent isotype controls. (G) Absolute numbers of $CD44^{lo}$ (naive) and $CD44^{hi}$ (memory) CD4 and CD8 cells per organ in the spleen (S) and inguinal lymph nodes (LN) of WT and Hq mice. *, $P < 0.01$; **, $P < 0.05$. All data are shown as mean ± SE ($n = 3–5$) and are representative of at least three independent experiments.

Published August 6, 2012

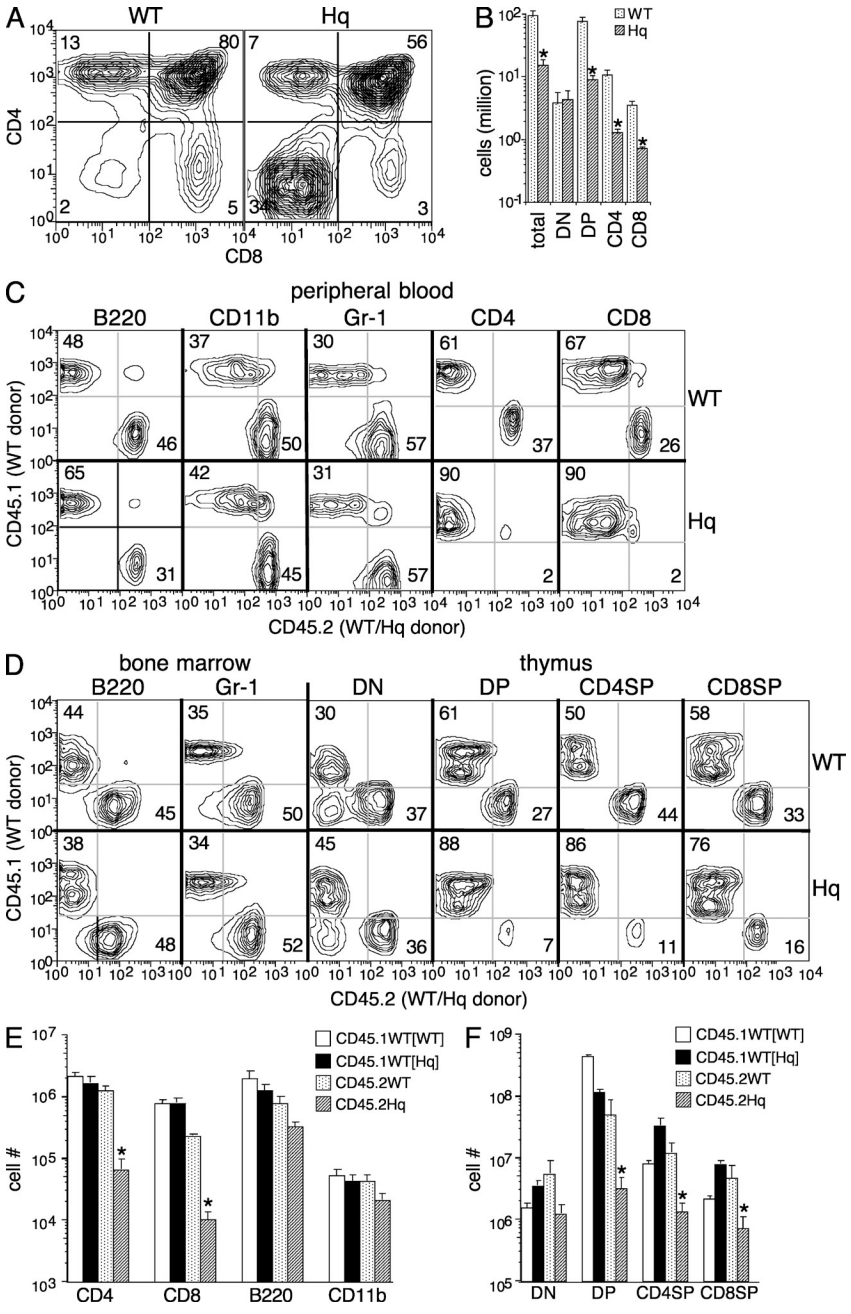

Figure 2. Thymus-specific T cell lineage–autonomous developmental blockade in Hq mice. (A) Representative analysis of thymocytes from 8–12-wk-old WT and Hq mice stained for CD4 and CD8, showing frequencies of cells in quadrants. Data are representative of three independent experiments. (B) Numbers of thymocyte subpopulations per thymus in WT and Hq mice, as mean ± SE ($n = 4$). *, $P < 0.01$. (C–F) Mixed bone marrow chimeric mice were constructed by giving CD45.1xCD45.2 F1 recipients WT CD45.1 bone marrow in a 1:1 ratio with CD45.2 WT or Hq marrow (as indicated). Chimeric mice were analyzed at 4–8 wk for the distribution of CD45 allotypes in various cell lineages in different tissues. Cells from chimeric mice were stained for donor CD45 allotypes and various lineage markers. Representative two-color plots are shown for peripheral blood cells stained for CD45 allotypes versus B220, CD11b, Gr-1, CD4, or CD8 (C), and bone marrow cells stained for CD45 allotypes versus B220 and Gr-1 and thymocytes stained for CD45 allotypes versus CD4 and CD8 (D). Frequencies of cells in each quadrant are indicated. Absolute numbers of lymph node CD4, CD8, B220, or CD11b cells (E) and of thymocyte DN, DP, CD4SP, and CD8SP subsets (F) of either CD45.1$^+$ or CD45.2$^+$ phenotype from the chimeric mice receiving either WT or Hq bone marrow as described. The groups shown are CD45.1 (WT donor) from chimeras given CD45.2 WT (CD45.1WT[WT]) or CD45.2 Hq (CD45.1WT[Hq]) marrow, and the CD45.2 cells from these chimeras (identified as CD45.2WT and CD45.2Hq). Data are shown as mean ± SE ($n = 3$). *, $P < 0.01$. Data are representative of five independent experiments.

Hq lineage cells to the DN compartment was equivalent, the Hq contribution declined notably in the succeeding DP and SP compartments (Fig. 2, D and F). These chimera-based data suggested that a relative lack of Aif specifically affects T lineage cells in cell-autonomous fashion and leads to attrition beyond the DN thymocyte stage in vivo.

the developmental alterations seen in Hq mice. For this, we made parent-F1 mixed bone marrow chimeras in which irradiated recipient mice were reconstituted with a mixture of bone marrow cells from CD45.1$^+$ WT and CD45.2$^+$ WT or Hq mice. Upon reconstitution, Hq donor marrow reconstituted CD4 and CD8 T cells in peripheral blood and lymph nodes very poorly, whereas this deficit was far less prominent in B cells, macrophages, and granulocytes (Fig. 2, C and E). Similarly, B220$^+$ B lineage cells and Gr-1$^+$ granulocytic lineage cells in the bone marrow of these chimeric mice showed little difference in the ability of WT and Hq donors to repopulate these compartments (Fig. 2 D). In the thymus of these mixed marrow chimeric mice, although the contribution of WT and

The thymic defect in Hq mice is most prominent at the β-selection stage

Within the DN thymocyte compartment, subpopulations as defined by their CD25/CD44 expression phenotype showed alterations in Hq thymi, most notably with reduced frequency of CD44$^+$CD25$^-$ DN1 cells, increased frequency of the CD44$^-$CD25$^+$ DN3 stage cells, and reduced frequency of the CD44$^-$CD25$^-$ DN4 population (Fig. 3, A and B). The transition from CD27$^-$DN3 to CD27$^+$DN3 stages, which accompanies successful entry into β-selection (Taghon et al., 2006), was also poor in Hq mice (Fig. 3, C and D).

We also tested Hq thymocytes in vitro by using the OP9DL1 stromal cell line expressing the Notch-1 ligand

Published August 6, 2012

Delta-1, which has been shown to support the development of the T cell lineage from undifferentiated precursors (Schmitt and Zúñiga-Pflücker, 2002; Schmitt et al., 2004). Early precursor thymocytes were purified from WT or Hq thymus by sorting, first by depletion of $CD4^+$, $CD8^+$, $CD3^+$, $B220^+$, $Gr\text{-}1^+$, $CD11b^+$ and $CD11c^+$, $NK1.1^+$, and TCR-γ/δ^+ cells, followed by positive selection to purify $CD44^+$ cells, to provide a starting population consisting of DN1, DN2, and early thymic precursors. The purity obtained for this population was >90%. These early thymocytes were cultured with OP9DL1 monolayers in the presence of IL-7 and Flt3L as previously described (Schmitt and Zúñiga-Pflücker, 2002). On day 3 of culture, Thy-1^+CD44^- cells were gated as the population that had undergone T cell lineage developmental progress and examined for the expression of CD25 to estimate the transition from the DN3 ($CD25^+$) to the DN4 ($CD25^-$) stage. It was evident that the Hq Thy-1^+CD44^- thymocytes had a far greater proportion of $CD25^+$ DN3 cells than did the WT cells (Fig. 3, E and G). No cells had reached DP stage maturation at this point.

However, the B cell lineage in Hq mice appeared normal. In addition to normal peripheral B cell numbers (Fig. 1 F), the developmental stages of the B cell lineage in the bone marrow of Hq mice showed normal frequencies and numbers, particularly at the pro–B-to-pre–B stage transition accompanying heavy chain selection, a process analogous to thymic β-selection (Fig. 3, H and J). Thus, a major thymic defect appears to be during the stage of β-selection during the transition to the DN4 and subsequent DP stages, with no corresponding defect at comparable stages of B cell development.

The Hq thymic defect is independent of TCR-β recombination and is associated with cell death during β-selection

We next tested if the major developmental checkpoint, namely, successful pre-TCR formation which initiates β-selection (Michie and Zúñiga-Pflücker, 2002), was compromised in Hq mice. Intracellular TCR-β–expressing DN3 cells from WT and Hq thymus showed equivalent frequencies (Fig. 4, A and B). We then directly tested if the Hq defect was dependent on impaired *tcrb* recombination by breeding the Hq mice with DO11.10-TCR transgenic (tg) mice to generate Aif hypomorphic mice expressing already recombined TCR-β and TCR-α chains. Hq-DO11.10 mice so generated continued to show thymic hypocellularity (Fig. 4 C). Thus, the data so far indicated that Aif hypomorphism led to a specific failure of β-selection independent of pre-TCR formation.

We next examined proliferation and cell death during β-selection. The frequencies of actively cycling cells in the DN3 and DN4 compartments, as detected by the in vivo incorporation of a pulse of 5-ethynyl-2′-deoxyuridine (EdU), were lower in Hq than in WT mice (Fig. 4, D and E). Also, Hq DN4 cells were smaller than those in WT mice (Fig. 4 D). Furthermore, DN cells in the Hq thymus showed significantly higher frequencies of annexin V–binding apoptotic

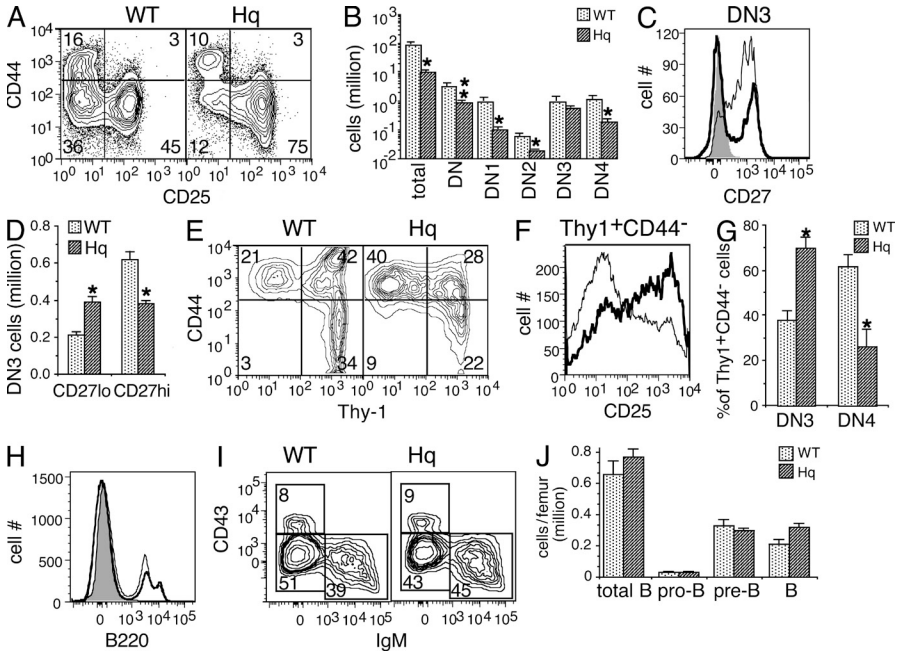

Figure 3. β-Selection stage thymic defect in Hq mice. (A) Representative analysis of CD44 and CD25 expression on gated DN thymocytes (negative for lineage markers CD3/CD4/CD8/B220/CD11b/CD11c/Gr-1) of 8–12-wk-old WT and Hq mice, showing frequencies of cells in quadrants. (B) Numbers of various thymocyte subsets per thymus in WT or Hq mice, from analyses as in A, shown as mean ± SE ($n = 3$). *, $P < 0.01$; **, $P < 0.05$. (C) Representative analysis of gated DN3 thymocytes from WT (thin line) or Hq (thick line) stained for CD27. Gray curve indicates isotype control. (D) Frequencies of $CD27^{lo}$ and $CD27^{hi}$ DN3 thymocytes from WT and Hq mice as indicated, from analyses as in C, shown as mean ± SE ($n = 3$). *, $P < 0.01$. (E–G) Magnetically sorted >90% pure DN1 + DN2 thymocytes from WT or Hq thymus were put in culture with the OP9DL1 stromal cell line. Cells were harvested and analyzed flow cytometrically on day 3 of culture. Two-color plots (E) show the expression profile of Thy-1 and CD44 on cells from WT or Hq cultures as indicated. Flow cytometric histograms (F) show the CD25 expression profile of gated Thy-1^+CD44^- cells from WT (thin line) or Hq (thick line) cultures. Bar diagrams (G) show frequencies of DN3 ($CD44^-CD25^+$) and DN4 ($CD44^-CD25^-$) cells in the Thy-1^+CD44^- compartment of WT or Hq cultures as mean ± SE ($n = 3$). *, $P < 0.05$. (H) B220 staining on bone marrow cells from WT (thin line) or Hq (thick line) mice. Filled histogram represents isotype control. (I) Representative two-color analysis of gated $B220^+$ bone marrow cells from WT or Hq mice, stained for CD43 and IgM, showing frequencies of pro–B ($CD43^+IgM^-$), pre–B ($CD43^-IgM^-$), and B ($CD43^-IgM^+$) cells. (J) Numbers of B cell lineage subsets in bone marrow of WT or Hq mice, from analyses in H and I, shown as mean ± SE ($n = 3$). Data are representative of at least two independent experiments.

Published August 6, 2012

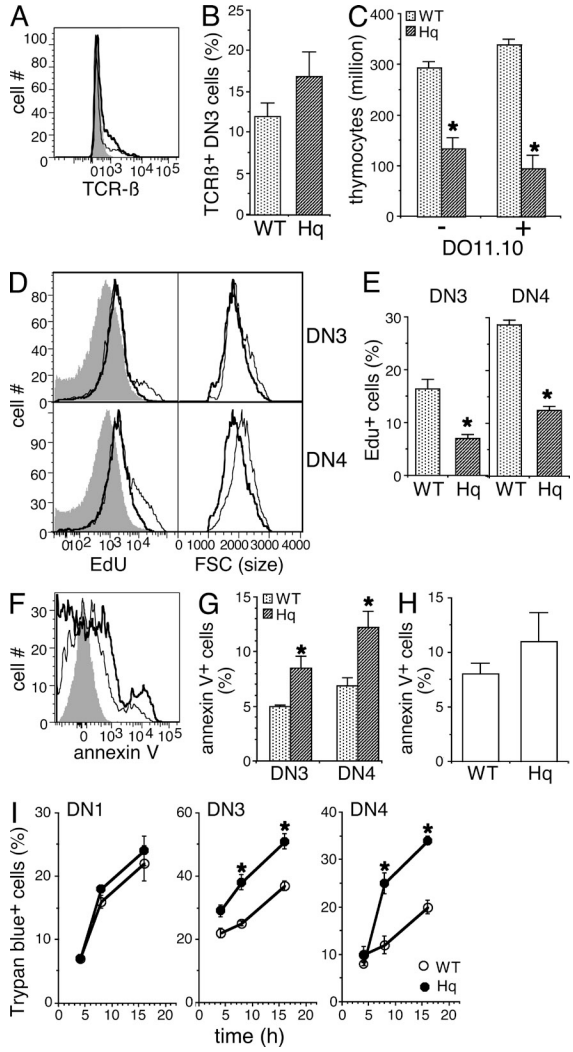

Figure 4. Hq thymic defect is independent of TCR-β recombination and associated with cell death during β-selection. (A) Representative histogram overlay of gated DN3 thymocytes from WT (thin line) or Hq (thick line) mice, stained for intracellular TCR-β. Filled histogram represents isotype control. (B) Frequencies of intracellular TCR-β containing DN3 thymocytes in WT and Hq mice as calculated from the analysis shown in A. Data are shown as mean ± SE (n = 3). (C) Total thymocyte numbers in 4–6-wk-old F2 progeny littermate mice from Hq and DO11.10-TCR tg parentage. F1 mice generated from Hq × DO11.10 breeding were intercrossed. The resultant progeny were typed for the Hq allele and the TCR transgene and separated into four groups on that basis as shown. Data are shown as mean ± SE (n = 3–4). *, P < 0.01. (D) Representative histogram overlays of gated DN3 and DN4 thymocytes from WT (thin line) or Hq (thick line) mice given EdU in vivo and stained for EdU incorporation. Both EdU staining and cell size (FSC) are shown. Filled histograms represent isotype controls. (E) Frequencies of DN3 and DN4 thymocytes incorporating EdU in vivo in WT and Hq mice as calculated from the analysis shown in D. Data are shown as mean ± SE (n = 3). *, P < 0.01. (F) Annexin V staining on gated DN thymocytes from WT (thin line) or Hq (thick line) mice. Filled histogram represents isotype control. (G) Frequencies of annexin V–binding DN3 and DN4 thymocytes in WT and Hq mice. Data are shown as mean ± SE (n = 4). *, P < 0.01. (H) Frequencies of annexin V–binding DP thymocytes in WT and Hq mice. Data are shown as mean ± SE (n = 3). (I) DN1, DN3, and DN4 thymocytes from WT or Hq mice as indicated were electronically sorted and put in culture in vitro. After varying periods of time as shown, the frequencies of dead cells were estimated by Trypan blue staining. Data are shown as mean ± SE (n = 3). *, P < 0.05. Data are representative of at least three independent experiments.

cells than those in the WT thymus (Fig. 4 F). DN3 and DN4 stage cells both showed evidence of greater annexin V–binding apoptotic cells in Hq than in WT thymi (Fig. 4 G), whereas the frequency of apoptotic cells was not significantly different in DP thymocytes of WT and Hq mice (Fig. 4 H). Furthermore, when DN1, DN3, and DN4 thymocytes were purified by electronic sorting and cultured for up to 16 h, DN3 and DN4 cells from Hq thymi showed higher frequencies of cell death (Fig. 4 I). Although DN1 thymocyte frequencies were reduced in Hq mice, DN1 thymocytes from WT and Hq mice showed comparable death in cultures in vitro (Fig. 4 I). Together, these data suggest a specific and prominent intrathymic defect in Hq mice at the β-selection stage associated with enhanced cell death.

T cell developmental defect in Aif-hypomorphic mice is corrected by tg Aif

If the thymic defect we have observed in Hq mice was truly a consequence of Aif hypomorphism, then provision of additional Aif in the Hq background should correct the defect. For testing this, we generated tg mice that express Aif using a heterologous promoter (Fig. 5 A). According to the testicular transgenesis protocol reported earlier (Dhup and Majumdar, 2008), we injected linearized plasmid DNA intratesticularly in FVB/J male mice followed by electroporation in vivo. The male mice were then bred with FVB/J females to obtain tg progeny (Fig. 5 B). Independent founder lines were obtained. Transgene-bearing male founder mice were then bred with heterozygous Hq females to generate male littermates of all four genotypes, namely, non-tg WT, non-tg Hq, tg WT, and tg Hq. Both the transgene and Hq status were confirmed by genotyping PCRs. Western blot analysis of splenic cells from the four genotypes showed that the tg Hq mice had enhanced levels of Aif, although they were still not comparable to the non-tg WT mice (Fig. 5 C).

We next compared the T cell lineage phenotype in littermate mice of the four genotypes identified in the previous paragraph. The additional expression of tg Aif in WT mice did not have any detectable effect in any of the readouts used. In the spleen, the reduced frequencies of CD4 and CD8 T cells, and even more specifically of naive CD44^{lo} cells, found in Hq mice were increased in the tg Hq mice (Fig. 5, D and E). Similarly, the thymic hypocellularity found in Hq mice was significantly corrected in tg Hq mice (Fig. 5 F). The high DN thymocyte frequency found in Hq mice was reduced in the tg Hq mice (Fig. 5 G), and the altered frequencies of DN3 and DN4 cells, as well as the smaller size of DN4 cells, were

Published August 6, 2012

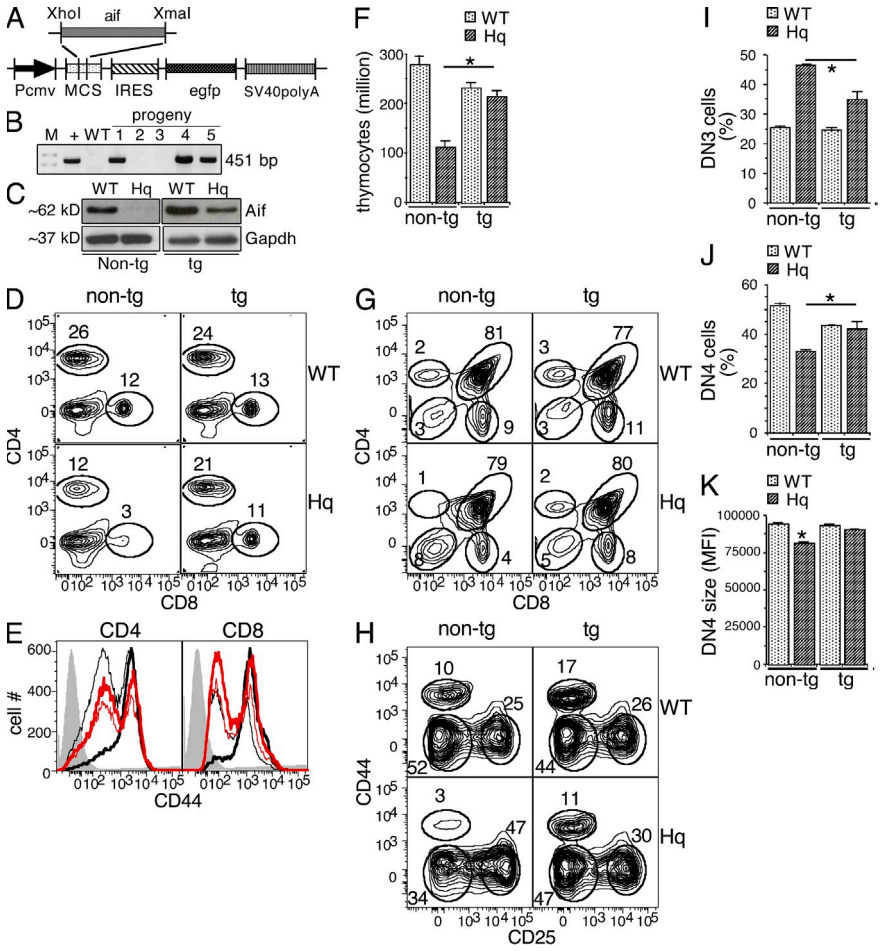

Figure 5. Restoration of normal thymic development and peripheral T cell phenotype in Hq mice by transgenically expressed Aif. (A) Plasmid map for the expression vector used for generating aif tg mice. (B) PCR results of screening for transgene inheritance on genomic DNA from ear clip tissue from the progeny of male mice receiving intratesticular injection of the plasmid shown in A. The vector control (+), a WT mouse DNA sample, and five sample progeny mouse samples are shown, along with a marker lane (M). (C) Western blot analysis of Aif expression in spleen cell lysates. Transgene-bearing male mice were bred with heterozygous Hq females to generate male littermates of all four genotypes, namely, non-tg WT, non-tg Hq, tg WT, and tg Hq, as indicated. (D) Representative two-color analyses of splenic cells from 6–8-wk-old WT and Hq mice of either non-tg or tg genotypes as indicated, stained for CD4 and CD8, showing frequencies of CD4 and CD8 cells. (E) Representative analysis of CD44 levels on gated CD4 or CD8 cells from spleen of WT (black lines) or Hq (red lines) mice of either non-tg (thin lines) or tg (thick lines) genotypes as shown. Filled histograms represent isotype controls. (F) Numbers of total thymocytes per thymus in 6–8-wk-old WT and Hq mice of either non-tg or tg genotypes as indicated, as mean ± SE ($n = 3$). *, $P < 0.01$. (G) Representative analysis of thymocytes from WT and Hq mice of either non-tg or tg genotypes as indicated, stained for CD4 and CD8, showing frequencies of subpopulations. (H) Representative analysis of CD44 and CD25 expression on gated DN thymocytes (negative for lineage markers CD3/CD4/CD8/B220/CD11b/CD11c/Gr-1) of WT and Hq mice of either non-tg or tg genotypes as indicated, showing frequencies of DN thymocyte subpopulations. (I–K) Frequencies of DN3 (I) and DN4 (J) thymocyte subsets, and mean size (as mean fluorescence intensity [MFI]) of DN4 thymocytes (K) from WT and Hq mice of either non-tg or tg genotypes as indicated, from analyses as in H, shown as mean ± SE ($n = 3$). *, $P < 0.01$. All flow cytometric analyses are representative of at least two independent experiments.

also substantively corrected in tg Hq mice (Fig. 5, H and K). Thus, an increase in the level of Aif per cell was sufficient to reverse the thymic defect in Hq mice.

Aif mediates its role in the thymus through its oxidoreductase function not its DNA-binding function

Aif is known to have a DNA-binding function essential for its proapoptotic activity (Ye et al., 2002), but it also has an oxidoreductase function that may be involved in its ability to regulate mitochondrial function, cell metabolism, and oxidative stress (Sevrioukova, 2011). Distinct point mutations in the mouse Aif protein selectively abrogate either the DNA-binding or the oxidoreductase function: K254A and R264A for abrogation of DNA-binding and T262A and V299A for abrogation of oxidoreductase activity (Maté et al., 2002; Ye et al., 2002; Urbano et al., 2005). We therefore examined if either or both functions were required to correct the Hq thymic defect. We generated these point mutant genes from the WT *aif* gene by site-directed mutagenesis and then generated tg mice that express these mutant Aif versions using the same heterologous promoter and testicular transgenesis protocol used in the previous section. tg progeny thus obtained were bred as described with heterozygous Hq females to generate male littermates of all four genotypes, namely, non-tg WT, non-tg Hq, tg WT, and tg Hq, for both mutant Aif molecules, namely, the Aif254/264 and the Aif262/299. Both the tg and Hq status were confirmed by genotyping PCRs. Western blot analysis of splenic cells showed that the tg-Hq mice had significant levels of Aif in both Aif254/264 tg and Aif262/299 tg mice, and the two transgenes did not show any notable differences in their expression levels (Fig. 6 A). Once again, as with the nonmutated Aif transgene shown in Fig. 5, the levels of transgene expression did not match the levels of endogenous Aif expression in non-tg WT mice.

We next compared the T cell lineage phenotype in littermate mice of the four genotypes identified for both

Published August 6, 2012

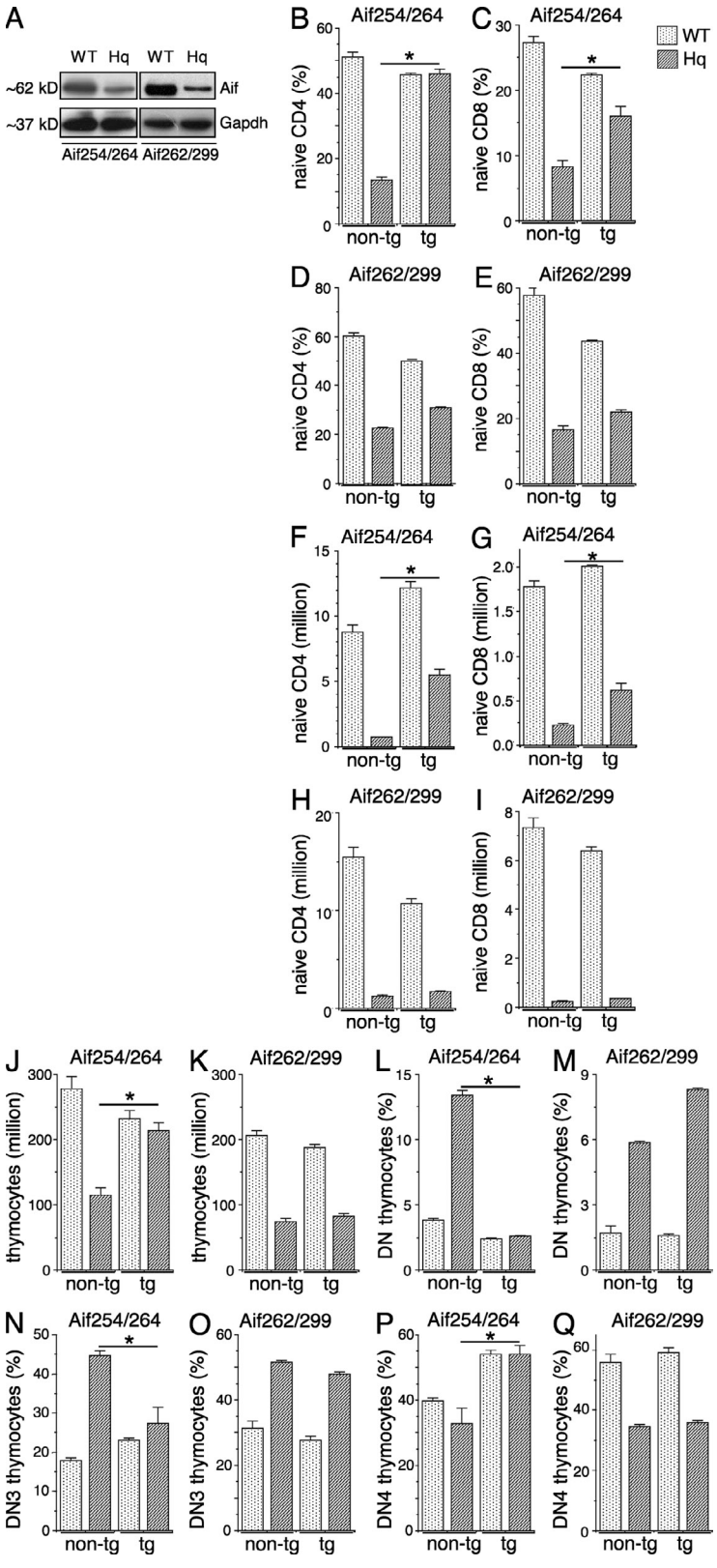

Figure 6. Restoration of normal thymic development and peripheral T cell phenotype in Hq mice requires the oxidoreductase function but not the DNA-binding function of Aif. (A) Western blot analysis of Aif expression in spleen cell lysates. Mice bearing transgenes encoding the mutant Aif constructs Aif254/264 or Aif262/299 were bred with heterozygous Hq females to generate male tg WT and tg Hq littermates as shown, and spleen cell lysates were tested. (B–E) Frequencies of naive CD4 (B and D) and naive CD8 (C and E) cells in spleens from 6–8-wk-old WT and Hq littermate mice of either non-tg or tg genotypes (with either Aif254/264 or Aif262/299 as indicated) as shown, as mean ± SE ($n = 3$). *, $P < 0.01$. (F–I) Numbers per spleen of naive CD4 (F and H) and naive CD8 (G and I) cells in WT and Hq littermate mice of either non-tg or tg genotypes (with either Aif254/264 or Aif262/299 as indicated) as shown, as mean ± SE ($n = 3$). *, $P < 0.01$. (J and K) Numbers of thymocytes from 6–8-wk-old WT and Hq littermate mice of either non-tg or tg genotypes (with either Aif254/264 or Aif262/299 as indicated) as shown, as mean ± SE ($n = 3$). *, $P < 0.01$. (L–Q) Frequencies of DN (L and M), DN3 (N and O), and DN4 (P and Q) thymocytes from WT and Hq littermate mice of either non-tg or tg genotypes (with either Aif254/264 or Aif262/299 as indicated) as shown, as mean ± SE ($n = 3$). *, $P < 0.01$. All flow cytometric analyses are representative of at least two independent experiments.

Aif254/264 and Aif262/299. The tg expression of either of these Aif mutant proteins in WT mice did not have any detectable effect in any of the readouts used. In the spleen, the reduced frequencies and numbers of naive CD4 and CD8 T cells found in Hq mice were increased in Aif254/264 tg Hq mice but not in Aif262/299 tg Hq mice (Fig. 6, B and I), although the recovery seen with Aif254/264 was not as complete as that observed with WT Aif (Fig. 5). Similarly, the thymic hypocellularity found in Hq mice was significantly corrected in Aif254/264 tg Hq mice but not in Aif262/299 tg Hq mice (Fig. 6, J and K). The high DN thymocyte frequency found in Hq mice was reduced (Fig. 6, L and M) and the altered frequencies of DN3 and DN4 cells were substantively corrected in Aif254/264 tg Hq mice but not in Aif262/299 tg Hq mice (Fig. 6, N and Q). It remains formally possible that higher levels of expression of the Aif262/299 transgene would eventually lead to rescue of the thymic defect. However, the data do suggest that the oxidoreductase function of Aif may be required for maintaining normal thymic development, whereas the DNA-binding function is likely to be dispensable.

Aif hypomorphism leads to thymic hypocellularity through ROS regulation

The possibility of a requirement for the oxidoreductase function of Aif in correcting the Hq thymic defect indicated that the defect could be a result of ROS stress in Aif-hypomorphic thymocytes. We therefore tested this in an independent pharmacological approach by examining whether treatment with a cell-permeable antioxidant that could mimic both superoxide dismutase (SOD) and catalase, namely Euk-134 (Doctrow et al., 2002),

Published August 6, 2012

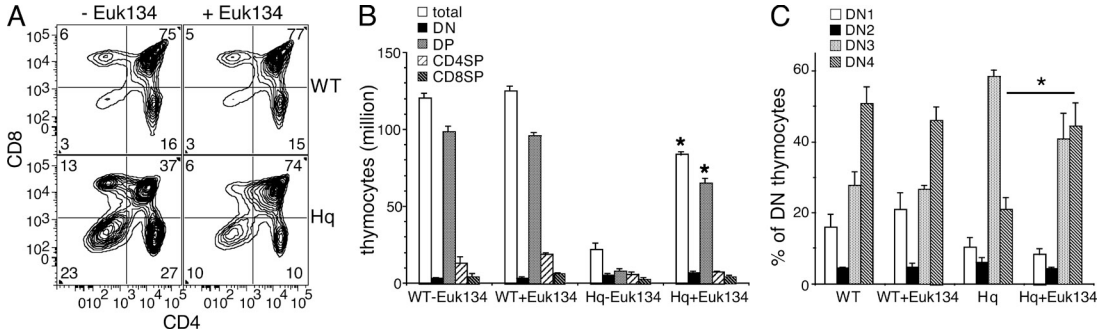

Figure 7. Increased ROS levels are involved in the thymic hypocellularity of Hq mice. (A) Representative two-color CD4 versus CD8 analysis of thymocytes from WT or Hq mice treated in vivo with Euk-134, as indicated. Frequencies of cells in each quadrant are shown. (B) Absolute numbers per thymus of total thymocytes and subsets as indicated in WT and Hq mice treated in vivo with Euk-134. Data are shown as mean ± SE (n = 3–4). *, $P < 0.05$. (C) Frequencies of DN thymocyte subsets as indicated in WT and Hq mice treated in vivo with Euk-134. Data are shown as mean ± SE (n = 3–4). Data are representative of three independent experiments.

affected the Hq thymic defect in vivo. Young (2 wk old) WT and Hq mice were treated daily with Euk-134 or vehicle alone for 14 d before the thymic phenotype was determined. Euk-134 treatment made no discernible difference to WT thymic cellularity or subpopulation frequencies, but in Hq mice, Euk-134 decreased the DN thymocyte frequency and significantly improved total thymic cellularity, particularly that of the DP population (Fig. 7, A and B). Euk-134 treatment also increased the DN4 frequency in Hq mice (Fig. 7 C). Together, these data indicate that Aif regulates the efficiency of transition through β-selection, probably by using its catalytic function to control oxidative stress.

We next directly tested if Hq DN thymocytes show higher levels of oxidative stress. The peroxide-sensitive dye 2′-7′-dichlorofluorescein diacetate (DCFDA) indicated higher ROS levels in Hq than in WT DN3 and DN4 cells (Fig. 8 A). Consistent with this, Hq DN3 and DN4 thymocytes showed lower levels of reduced glutathione, as reflected by lower intensities of staining by monochlorobimane (mBCl; Hedley and Chow, 1994; Fig. 8 B). However, the superoxide-sensitive dye MitoSOX red did not show such a difference in DN3 and DN4 cells (Fig. 8 C),

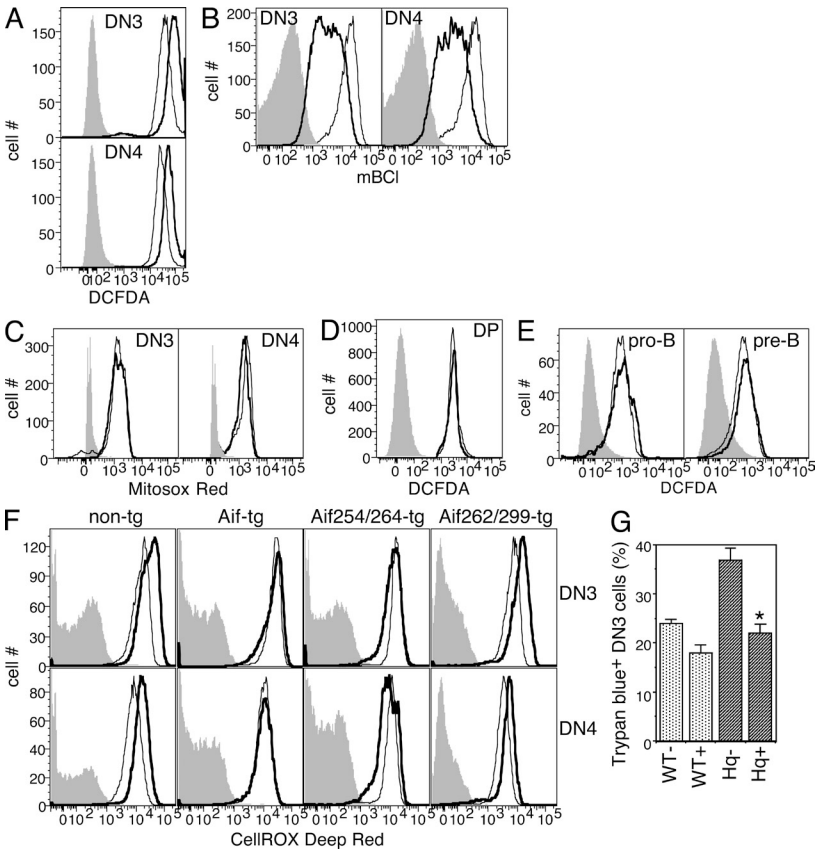

Figure 8. Increased ROS levels are involved in the thymic hypocellularity of Hq mice. (A–C) Representative histogram overlays of gated DN3 and DN4 thymocytes from WT (thin lines) or Hq (thick lines) mice stained with DCFDA (A), mBCl (B), or MitoSOX red (C) as indicated. Filled histograms represent isotype controls. (D) Representative histogram overlays of gated DP thymocytes from WT (thin lines) or Hq (thick lines) mice stained with DCFDA. Filled histogram represents negative control. (E) Representative histogram overlays of gated $B220^+CD43^+IgM^-$ pro–B or $B220^+CD43^-IgM^-$ pre–B cells from bone marrow of WT (thin lines) or Hq (thick lines) mice stained with DCFDA. Filled histograms represent negative controls. (F) Representative histogram overlays of gated DN3 and DN4 thymocytes from WT (thin lines) or Hq (thick lines) mice which were non-tg, Aif tg, Aif254/264 tg, or Aif262/299 tg as indicated, stained with the ROS indicator dye CellROX Deep Red. Filled histograms represent negative controls. Data represent three to eight independently tested littermate pairs. (G) DN3 thymocytes from WT or Hq mice as indicated were electronically sorted and put in culture in vitro for 8 h with (−) or without (+) Euk-134 as indicated, and the frequencies of dead cells were estimated by Trypan blue staining. Data are shown as mean ± SE (n = 3) *, $P < 0.01$. All data are representative of at least two independent experiments.

Published August 6, 2012

suggesting that Hq thymocytes suffer from peroxide stress. Although DP thymocytes from Hq mice did show an increase over WT cells in DCFDA staining levels, this was far more modest than in DN3/DN4 cells (Fig. 8 D). Thus, low levels of Aif lead to higher oxidative stress in DN thymocytes. In contrast, the closely related B cell lineage does not show any differences in ROS levels between Hq and WT bone marrow as indicated by DCFDA staining (Fig. 8 E).

A further prediction was that this enhancement of ROS levels in non-tg DN3/DN4 Hq thymocytes would no longer be seen in thymocytes of Hq mice carrying either the WT Aif transgene or the DNA-binding–deficient Aif254/264 transgene used in Figs. 5 and 6 but would continue to be apparent in the thymocytes of mice carrying the oxidoreductase–deficient Aif262/299 transgene. Because the transgene contains enhanced GFP (eGFP), it was not appropriate to use DCFDA to measure ROS levels. We therefore used an alternate ROS-sensitive dye, CellROX Deep Red, to examine ROS level differences in DN3 and DN4 thymocytes of all three tg lines. Consistent with the data on rescue of thymic cellularity, the WT Aif transgene does indeed abrogate the higher ROS levels in DN3 and DN4 thymocytes as does the Aif254/264 mutant with abrogated DNA-binding function, whereas the mutant Aif262/299 with abrogated oxidoreductase function does not do so (Fig. 8 F).

Finally, we tested the prediction that Euk-134, which rescues the Hq thymic defect in vivo, provides protection from the enhanced cell death seen in Hq DN thymocytes. When electronically sorted WT or Hq DN3 and DN4 thymocytes were put in culture with or without Euk-134 for 8 h, the enhanced death seen in Hq DN3 and DN4 thymocytes was inhibited by Euk-134 (Fig. 8 G).

DISCUSSION

Using the Aif-hypomorphic Hq strain of mice, we have previously shown major alterations in the sensitivity of activated peripheral Hq T cells to both NID and to activation-induced cell death in vitro (Srivastava et al., 2007). We now demonstrate that these mice also show notable changes in the T cell compartment in vivo. Specifically, our data indicate that Aif hypomorphism in T lineage cells leads to a reduction in the efficiency of developmental transition from the DN to the DP thymocyte stage, showing that Aif plays a major role in regulating the development of T cells.

Hq mice have fewer numbers of peripheral T cells, particularly naive phenotype cells. Curiously, the numbers of $CD44^{hi}$ memory phenotype T cells are almost comparable between WT and Hq mice. In the absence of functional evidence for the memory status of the $CD44^{hi}$ T cells in Hq mice, it remains possible that, in a lymphopenic environment in Hq mice, naive thymic emigrants would undergo continual homeostatic expansion, which might alter their CD44 phenotype as has been observed in some instances (Cho et al., 2000). Nonetheless, our data are consistent with previous indications that impaired NID of activated T cells is associated with a preferential survival of memory T cells (Hildeman, 2004; Vig et al., 2004).

The low frequency of T cells in the periphery of Hq mice is also seen in the mixed bone marrow chimeras. It is specific to the T cell lineage because macrophage and B cell development does not appear to be drastically affected. Furthermore, it is accompanied by notable alterations in thymic development. The thymus is hypocellular in Hq mice, and the numbers of DP and CD4/CD8SP thymocytes are greatly reduced in them. The numbers of DN thymocytes are far less drastically reduced. In fact, in some experiments, particularly in younger Hq mice, DN thymocyte numbers are comparable between Hq and WT mice. These findings are also observed in mixed bone marrow chimeras, in which the numbers of DN thymocytes of WT and Hq origin are comparable, whereas the numbers of DP thymocytes of Hq origin are drastically lower. Thus, Hq mice have a T lineage cell-autonomous defect in the DN-DP transition in the thymus.

The cellularity of the thymus, particularly the number of DP thymocytes, is significantly controlled by the proliferation of developing DN thymocytes (Dudley et al., 1994). The relevant DN stage subpopulations show significant alterations in Hq mice. Although DN1 cell frequencies and numbers are reduced, DN3 cell frequencies are increased in Hq mice and their numbers are comparable between Hq and WT mice. In contrast, DN4 cell frequencies and numbers are reduced in Hq mice. In fact, Hq DN3 cells show a poor transition between $CD27^-$ and $CD27^+$ stages, and $CD27^-$ DN3 cell numbers are higher in Hq compared with WT mice. Even when $DN1^+DN2$ thymocytes are put onto OP9-DL1 stromal cells in maturation cultures in vitro, the DN3-DN4 transition is poor in Hq cells. Thus, a major defect in the Hq thymus appears to become manifest at the point of transition from the DN3 to the DN4 stage.

Two major events are involved in the process of β-selection: the successful formation of pre-TCRs upon productive recombination at the TCR-β locus, and the transduction of signals through the pre-TCR to induce proliferation as well as developmental transition (Wiest et al., 1999; Michie and Zúñiga-Pflücker, 2002). The formation of the pre-TCR depends on the successful recombination of the TCR-β locus (Dudley et al., 1994). DN thymocytes from Hq and WT mice show comparable frequencies of intracellular TCR-β protein-expressing cells. Furthermore, the tg provision of an already recombined set of TCR genes does not rescue the thymic hypocellularity in the Hq genotype. Thus, the thymic β-selection defect in Hq mice is likely to occur during the pre-TCR–driven events of proliferation and differentiation. This is supported by the finding that DN3 as well as DN4 cells in the Hq thymus proliferate poorly. Interestingly, the Hq DN4 cells also show a smaller mean size, suggesting that many cycling DN4 cells may be dying. In contrast, annexin V–binding apoptotic cell frequencies are increased in the Hq DN3 and DN4 populations, and Hq DN3 and DN4 cells (but not DN1 cells) show enhanced cell death in culture in vitro. The finding that the γ/δ T cell lineage is relatively unaffected in Hq mice is also consistent with the possibility that the proliferative step in β-selection of developing α/β T cells is particularly vulnerable to Aif hypomorphism.

Published August 6, 2012

Although we have used the Hq mouse strain reported to be hypomorphic for Aif, it was essential to obtain formal evidence that it was the *aif* hypomorphism that was, in fact, responsible for the T cell developmental defect we have observed. Strikingly, when we provide tg WT Aif in the Hq genotype, all features of T cell developmental defect reported here are substantially rescued, from the peripheral naive T cell numbers to the thymic cellularity and the DN3-DN4 thymocyte transition. Together, our observations therefore support a model in which an antiapoptotic function of Aif is required for successful survival of pre-TCR–expressing DN3 thymocytes as they proliferate and differentiate to the DN4 and DP stages.

What is the possible mechanism of the role of Aif in the DN3-DN4-DP progression downstream of the pre-TCR? Together, our data suggest that cells undergoing proliferative expansion during β-selection are dying, leading to reduction in the numbers of survivors that make it through to the DP stage. The antiapoptotic role of Aif has been very prominent in several cell lineages in vivo, from neurons (Ishimura et al., 2008) and muscle cells (Joza et al., 2005) to β cells in the islets of Langerhans (Schulthess et al., 2009). At least in neurons, there is reason to believe that Aif hypomorphism leads to death during cell cycle (Klein et al., 2002; Ishimura et al., 2008) and that this is related to alterations in the assembly of the mitochondrial oxidative phosphorylation apparatus and/or the generation and handling of oxidative stress (Vahsen et al., 2004). Although Aif was proposed to be a hydrogen peroxide scavenger (Klein et al., 2002), it has many more complex roles in mitochondrial functions, many of which lead to the generation of oxidative stress in the absence of Aif (Vahsen et al., 2004; Cheung et al., 2006; Joza et al., 2009).

The role of the cellular redox status in developing T cells has been reported to be a major factor in determining the efficiency of T cell development (Ivanov et al., 1993). It is therefore plausible that a similar susceptibility is created in DN thymocytes through similar mechanisms by Aif hypomorphism. The finding that γ/δ T cell numbers are not altered in Hq mice is consistent with this possibility because γ/δ selection is known to induce much less proliferation than β-selection (Passoni et al., 1997). On this background, we have examined the mechanism by which Aif hypomorphism caused disruption of T cell β-selection using both genetic and pharmacological tools. Provision of tg DNA-binding–deficient mutant Aif rescued the Hq thymic defect, whereas the oxidoreductase-deficient mutant Aif did not do so. As noted, because our Aif transgene expression levels do not reach those of endogenous Aif, it remains formally possible that higher levels of expression of the Aif262/299 mutant would lead to rescue of the thymic defect. Precise regulation of levels of Aif expression in the absence of knockin mice is a difficult problem because there is evidence that strong overexpression of Aif can lead to death of even transfected cell lines in culture, possibly as a result of spontaneous leakage of Aif from mitochondria (Loeffler et al., 2001; Urbano et al., 2005). Instead, we have tried to test the predictions arising from the likely requirement for the oxidoreductase function of Aif using an independent pharmacological approach with the SOD/catalase mimic Euk-134. Treatment of Hq mice in vivo with this SOD/catalase mimic rescued both the thymic defect and the enhanced DN3 and DN4 cell death in vitro, and Hq DN thymocytes showed high ROS levels. These high ROS levels in Hq mice were abrogated by the WT Aif transgene, as well as by the DNA-binding–deficient Aif254/264 transgene, but not by the oxidoreductase-deficient Aif262/299 transgene. Thus, Aif-deficient thymocytes are defective in the efficiency of β-selection as the result of a failure to handle ROS stress leading to enhanced cell death and reduced proliferation.

Curiously, despite the ubiquitous expression of Aif in all cell lineages, Aif hypomorphism causes tissue-specific defects (Klein et al., 2002). Similarly, because we observe a thymic defect, the B cell lineage shows no heavy chain selection defect in Hq mice, raising the question of the cell type specificity of this defect because proliferation during heavy chain selection in the B cell lineage is as substantial as during thymic β-selection (Kitamura et al., 1992). Consistent with our model of a connection between ROS stress and tissue defects in Aif hypomorphism, B lineage cells in Hq mice show no evidence of enhanced ROS stress, suggesting that the T cell lineage, which uses ROS for developmental signaling (Ivanov et al., 1993; Moon et al., 2004), is more susceptible to the effects of Aif hypomorphism than the B cell lineage is. This may address the lineage and tissue specificity of dysfunctional phenotypes observed in mice hypomorphic for a ubiquitously expressed protein like Aif. The utility and mechanisms for the generation and handling of oxidative stress in B versus T lineage cells thus now become issues of interest. Finally, our data also raise the question of whether this T lineage defect is observed in instances of human *aif* mutations leading to neuromuscular disease (Ghezzi et al., 2010) and, if it is, whether it has clinical implications of significance to the natural history of the disease.

MATERIALS AND METHODS

Aif constructs. The AIF-expressing plasmids used had a backbone of pIRES2-EGFP (Takara Bio Inc.) into which the WT mouse *aif* cDNA (gift from S. Ackerman, The Jackson Laboratory, Bar Harbor, ME) was cloned. Two different mutant forms of Aif with point mutations abrogating either the DNA-binding or oxidoreductase function were generated in this construct by site-directed mutagenesis. For this purpose, forward and reverse primers containing the mutant sequence were designed. Phusion polymerase (Thermo Fisher Scientific) with high fidelity and high processivity was used to amplify the entire construct using the mutated primers. After amplification, WT template strands were digested from the product by DpnI (New England Biolabs) and mutant sequence–containing DNA used to transform competent *Escherichia coli* cells. Colonies obtained were screened by sequencing to determine the presence of the desired mutation. Because each mutant required two point mutations, plasmids from the clones positive for the first mutation were used for a second round of mutation using appropriate primers. The mutations induced and the primers used were as follows: Aif254/264, K254A (5′-CAGATTACCTTTGAAGCGTGCTTGATTGCAACG-3′ and 5′-CGTTGCAATCAAGCACGCTTCAAAGGTAATCTG-3′) and R264A (5′-CGGGAGGCACTCCAGCAAGTCTGTCTGCCATC-3′ and 5′-GATGGCAGACAGACTTGCTGGAGTGCCTCCCG-3′); and Aif262/299, T262A (5′-GATTGCAACGGGAGGCGCTCCAAGAAGTCTGTCTGC-3′ and 5′-GCAGACAGACTTCTTGGAGCGCCTCCCGTTGCAATC-3′) and V299A (5′-GGAGAAGATCTCTCGGGAGGCCAAGTCAATTACAGTTATCG-3′ and 5′-CGATAACTGTAATTGACTTGGCCTCCCGAGAGATCTTCTCC-3′).

Published August 6, 2012

Mice. Hq mice (B6CBACa *A$^{w\text{-}J}$/A-Pdcd8^{Hq}*/J; The Jackson Laboratory) are in a mixed B6xCBA/CaJ background, and hence experiments described here have used normal littermates as WT controls. Also, because the *aif* gene is on the X chromosome, hemizygous males, either WT or Hq, were used. C57BL/6, B6.SJL, CBA/CaJ, and the DO11.10-TCR tg mice (The Jackson Laboratory) were bred in the Small Animal Facility of the National Institute of Immunology, New Delhi, India. All animal experiments were done with the approval (IAEC 240/10) of the Institutional Animal Ethics Committee of the National Institute of Immunology.

For treatment in vivo with the SOD and catalase mimic Euk-134, mice were given 10 mg/kg Euk-134 (Cayman Chemical) in normal saline (or normal saline alone) once daily intraperitoneally for 14 d. On day 15, thymocytes were isolated and stained for various cell surface markers for flow cytometry.

For breeding the TCR transgenes onto comparable WT or Hq backgrounds, TCR tg male mice were mated with homozygous Hq females. The F1 progeny were then intercrossed to obtain littermate mice that were WT non-TCR tg, Hq non-TCR tg, WT TCR tg, or Hq TCR tg. TCR transgene inheritance was confirmed by flow cytometric analysis of peripheral blood for the frequency of tg TCR expression in T cells. The Hq allele was typed by genomic PCR analysis as described by The Jackson Laboratory. Mice were euthanized at 6–8 wk of age for flow cytometric analysis of various tissues.

Mice transgenically expressing WT or mutant Aif were generated by the testicular transgenesis method (Dhup and Majumdar, 2008). The transgenes were constructed by cloning either the WT mouse *aif* cDNA sequence, or the Aif254/264 or Aif262/300 mutants generated by site-directed mutagenesis, into the IRES-eGFP plasmid which uses a CMV promoter (Takara Bio Inc.). The linearized plasmid was injected (150 ng/µl) at three separate testicular sites (10 µl/site) in each testis in anesthetized 4-wk-old FVB/J male mice as described. Electroporation was done by administration of eight square 40-V electric pulses in with a change in polarity after four pulses with a time constant of 0.05 s and an inter-pulse interval of ~1 s via an electric pulse generator (ECM2001; Harvard Apparatus) using a pair of sterile tweezer-type electrodes externally. 1 mo after electroporation, the mice were put into breeding with FVB/J females. The litters obtained were screened for transgene presence by performing PCR with primers designed across the IRES (forward primer: 5′-CTCTCCTCAAGCGTATTC-3′) and eGFP (reverse primer: 5′-GGACTTGAAGAAGTCGTG-3′) sequences of the construct. Transgene-expressing male progeny were then used for breeding with heterozygous Hq females to obtain male progeny of all four genotypes, namely, non-tg WT, tg WT, non-tg Hq, and tg Hq.

Bone marrow chimeras. For generation of mixed bone marrow chimeras, F1 mice generated by crossing B6.SJL (CD45.1) with CBA/CaJ (CD45.2) were used as recipients. 12 h after irradiation (400 rads with a Co^{60} source), a 1:1 mixture of 20×10^6 bone marrow cells from B6.SJL (CD45.1) mice and either WT or Hq mice (CD45.2) was given intravenously. Between 4 and 8 wk later, frequencies of endogenous and donor repopulating cells were scored using CD45.1- and CD45.2-specific markers by flow cytometry.

Flow cytometry. For enumeration of frequencies of CD4 and CD8 cells and their activation status, splenic and lymph node cells were stained for multicolor analysis for CD4, CD8, and CD44. Proportion of thymic subpopulations was analyzed in two-color analyses after staining them for CD4 and CD8. For analysis of DN subpopulations in the thymus, a cocktail of biotinylated antibodies followed by labeled streptavidin was used to label and exclude all cells which were positive for any one or more of the following markers: CD3, CD4, CD8, B220, CD11b, CD11c, Gr-1, NK1.1, and TCR-γ/δ. After exclusion of these non-DN thymocytes, the residual DN population was further analyzed for CD25 and CD44 frequencies using other fluorophores.

For analysis of bone marrow chimeric mice, cells were stained in multicolor analyses for CD45.1, CD45.2, and B, T, macrophage, and granulocyte markers. For detection of intracellular proteins such as TCR-β in DN thymocytes, cells were first stained for various cell surface markers, fixed, and permeabilized with 0.03% saponin before being stained with antibodies against the intracellular protein targets. For staining with annexin V, cells were washed in PBS and stained with labeled annexin V in annexin V staining buffer per manufacturer's protocols (BD) for 20 min, diluted with staining buffer, and analyzed within 30 min of labeling. For DCFDA, CellROX Deep Red, MitoSOX red, and mBCl staining, cells were incubated in 5 µM DCFDA, 5 µM MitoSOX red, 4 µM mBCl, or 5 µM CellROX Deep Red in the dark for 10–30 min (Molecular Probes). Cells were then washed and stained for various cell surface markers. Complete medium was added, and cells were washed and kept in the dark until analysis. For EdU labeling of DNA in proliferating cells, mice were given 100 µg EdU in PBS intraperitoneally, and thymocytes were isolated 2 h later. Cells were first stained for surface markers, followed by fixation and permeabilization. They were then incubated for 30 min at room temperature in staining solution containing 100 µM Alexa Fluor 488–azide according to the manufacturer's protocols (Invitrogen). For all flow cytometric analyses, samples stained with appropriate isotype antibodies served as negative controls.

The antibodies used for staining, either biotinylated or directly coupled to various fluorochromes, as well as fluorochrome-coupled streptavidin, were variously sourced (BD; eBioscience). DN1, DN3, and DN4 thymocytes were purified by electronic sorting (FACSAria III; BD) as thymocytes negative for non–T lineage and mature T lineage markers (CD4, CD8, CD3, CD25, CD11b, CD11c, Gr-1, NK1.1, TCR-γ/δ, and B220) and $CD44^+CD25^-$ (DN1), $CD44^-CD25^+$ (DN3), or $CD44^-CD25^-$ (DN4) cells. Data acquisition was done either on an LSR (BD) or on a FACSAria I or FACSAria III flow cytometer and data analyzed using FlowJo software (Tree Star).

In vitro thymocyte development cultures. Thymocytes from Hq mice or WT littermates were first negatively selected by staining with biotinylated antibodies against CD4, CD8, CD3, CD25, CD11b, CD11c, Gr-1, NK1.1, TCR-γ/δ, and B220 using magnetic columns (Miltenyi Biotec) to purify DN thymocytes. Subsequently, the nonbinding cell population was stained with anti-CD44 antibody and positively selected to obtain >95% pure $CD44^+$ DN1/DN2 stage thymocytes. The bone marrow stromal cell line OP9 expressing the Notch ligand Delta-like 1 was a gift from J.C. Zuniga-Pflucker (University of Toronto, Canada). OP9-DL1 cells and DN1/DN2 cells were co-cultured in medium containing 10 ng/ml Flt-3–Ligand and 5 ng/ml IL-7. The medium was changed gently on day 2 and cytokines were replenished. Cells were harvested on day 3 of co-culture and stained for Thy-1, CD25, CD44, CD8, and CD4 to track the stage of differentiation by flow cytometry.

In vitro thymocyte death assay. WT or Hq DN1, DN3, and DN4 thymocytes purified by electronic sorting were cultured for varying periods of time in flat bottomed 96-well plates in DME with 10% FCS with or without 50 µM Euk-134, and cell death was scored using Trypan blue.

Statistical analyses. Data were analyzed using Student's *t* test.

We thank Mr. Inder Jit Singh for extensive help with animal breeding and maintenance. We are grateful to Prof. Ranjan Sen for insightful comments on the manuscript.

This work was supported in part by grants from the Department of Biotechnology (to S. Rath: BT/PR-14592/BRB/10/858/2010; to A. George: BT/PR10954/BRB/10/625/2008 and BT/PR12849/MED/15/35/2009; to V. Bal: BT/PR-10284/Med/29/59/2007 and BT/PR14420/Med/29/213/2010; to S.S. Majumdar: BT/HRD/35/01/01/2010) and the Department of Science and Technology, Government of India (to S.S. Majumdar, A. George, V. Bal, and S. Rath), and by the National Institutes of Health (to J.M. Durdik; RO3AI070312-01A2) and the Arkansas Biosciences Institute (to J.M. Durdik). The National Institute of Immunology is supported by the Department of Biotechnology, Government of India.

The authors affirm that they have no conflicts of interest to declare.

Author contributions: H. Banerjee, A. Das, and S. Srivastava helped in planning and performed most critical experiments, helped analyze data, helped write the manuscript, and share first authorship. H.R. Mattoo, K. Thyagarajan, J.K. Khalsa, and

S. Tanwar helped in planning and performed some critical experiments and helped analyze some data and write the manuscript. S.S. Majumdar and D.S. Das planned and performed critical experiments requiring key technology and expertise. A. George, V. Bal, J.M. Durdik, and S. Rath conceived the question and approach, planned experiments, analyzed data, wrote the manuscript, and share senior authorship.

Submitted: 9 February 2011
Accepted: 20 July 2012

REFERENCES

Bidère, N., and A. Senik. 2001. Caspase-independent apoptotic pathways in T lymphocytes: a minireview. *Apoptosis*. 6:371–375. http://dx.doi.org/10.1023/A:1011390103783

Candé, C., F. Cecconi, P. Dessen, and G. Kroemer. 2002. Apoptosis-inducing factor (AIF): key to the conserved caspase-independent pathways of cell death? *J. Cell Sci.* 115:4727–4734. http://dx.doi.org/10.1242/jcs.00210

Cheung, E.C.C., N. Joza, N.A.E. Steenaart, K.A. McClellan, M. Neuspiel, S. McNamara, J.G. MacLaurin, P. Rippstein, D.S. Park, G.C. Shore, et al. 2006. Dissociating the dual roles of apoptosis-inducing factor in maintaining mitochondrial structure and apoptosis. *EMBO J.* 25:4061–4073. http://dx.doi.org/10.1038/sj.emboj.7601276

Cho, B.K., V.P. Rao, Q. Ge, H.N. Eisen, and J. Chen. 2000. Homeostasis-stimulated proliferation drives naive T cells to differentiate directly into memory T cells. *J. Exp. Med.* 192:549–556. http://dx.doi.org/10.1084/jem.192.4.549

Cleverley, S., S. Henning, and D. Cantrell. 1999. Inhibition of Rho at different stages of thymocyte development gives different perspectives on Rho function. *Curr. Biol.* 9:657–660. http://dx.doi.org/10.1016/S0960-9822(99)80289-9

Costello, P.S., S.C. Cleverley, R. Galandrini, S.W. Henning, and D.A. Cantrell. 2000. The GTPase rho controls a p53-dependent survival checkpoint during thymopoiesis. *J. Exp. Med.* 192:77–85. http://dx.doi.org/10.1084/jem.192.1.77

Dhup, S., and S.S. Majumdar. 2008. Transgenesis via permanent integration of genes in repopulating spermatogonial cells in vivo. *Nat. Methods*. 5:601–603. http://dx.doi.org/10.1038/nmeth.1225

Doctrow, S.R., K. Huffman, C.B. Marcus, G. Tocco, E. Malfroy, C.A. Adinolfi, H. Kruk, K. Baker, N. Lazarowych, J. Mascarenhas, and B. Malfroy. 2002. Salen-manganese complexes as catalytic scavengers of hydrogen peroxide and cytoprotective agents: structure-activity relationship studies. *J. Med. Chem.* 45:4549–4558. http://dx.doi.org/10.1021/jm020207y

Doerfler, P., K.A. Forbush, and R.M. Perlmutter. 2000. Caspase enzyme activity is not essential for apoptosis during thymocyte development. *J. Immunol.* 164:4071–4079.

Dudley, E.C., H.T. Petrie, L.M. Shah, M.J. Owen, and A.C. Hayday. 1994. T cell receptor β chain gene rearrangement and selection during thymocyte development in adult mice. *Immunity*. 1:83–93. http://dx.doi.org/10.1016/1074-7613(94)90102-3

Ferri, K.F., E. Jacotot, J. Blanco, J.A. Esté, N. Zamzami, S.A. Susin, Z. Xie, G. Brothers, J.C. Reed, J.M. Penninger, and G. Kroemer. 2000. Apoptosis control in syncytia induced by the HIV type 1–envelope glycoprotein complex: role of mitochondria and caspases. *J. Exp. Med.* 192:1081–1092. http://dx.doi.org/10.1084/jem.192.8.1081

Ghezzi, D., I. Sevrioukova, F. Invernizzi, C. Lamperti, M. Mora, P. D'Adamo, F. Novara, O. Zuffardi, G. Uziel, and M. Zeviani. 2010. Severe X-linked mitochondrial encephalomyopathy associated with a mutation in apoptosis-inducing factor. *Am. J. Hum. Genet.* 86:639–649. http://dx.doi.org/10.1016/j.ajhg.2010.03.002

Hedley, D.W., and S. Chow. 1994. Evaluation of methods for measuring cellular glutathione content using flow cytometry. *Cytometry*. 15:349–358. http://dx.doi.org/10.1002/cyto.990150411

Hildeman, D.A. 2004. Regulation of T-cell apoptosis by reactive oxygen species. *Free Radic. Biol. Med.* 36:1496–1504. http://dx.doi.org/10.1016/j.freeradbiomed.2004.03.023

Hoffman, E.S., L. Passoni, T. Crompton, T.M. Leu, D.G. Schatz, A. Koff, M.J. Owen, and A.C. Hayday. 1996. Productive T-cell receptor β-chain gene rearrangement: coincident regulation of cell cycle and clonality during development in vivo. *Genes Dev.* 10:948–962. http://dx.doi.org/10.1101/gad.10.8.948

Ishimura, R., G.R. Martin, and S.L. Ackerman. 2008. Loss of apoptosis-inducing factor results in cell-type-specific neurogenesis defects. *J. Neurosci.* 28:4938–4948. http://dx.doi.org/10.1523/JNEUROSCI.0229-08.2008

Ivanov, V., M. Merkenschlager, and R. Ceredig. 1993. Antioxidant treatment of thymic organ cultures decreases NF-kappa B and TCF1(α) transcription factor activities and inhibits α β T cell development. *J. Immunol.* 151:4694–4704.

Izquierdo, M., A. Grandien, L.M. Criado, S. Robles, E. Leonardo, J.P. Albar, G.G. de Buitrago, and C. Martínez-A. 1999. Blocked negative selection of developing T cells in mice expressing the baculovirus p35 caspase inhibitor. *EMBO J.* 18:156–166. http://dx.doi.org/10.1093/emboj/18.1.156

Joza, N., S.A. Susin, E. Daugas, W.L. Stanford, S.K. Cho, C.Y. Li, T. Sasaki, A.J. Elia, H.Y. Cheng, L. Ravagnan, et al. 2001. Essential role of the mitochondrial apoptosis-inducing factor in programmed cell death. *Nature*. 410:549–554. http://dx.doi.org/10.1038/35069004

Joza, N., G.Y. Oudit, D. Brown, P. Bénit, Z. Kassiri, N. Vahsen, L. Benoit, M.M. Patel, K. Nowikovsky, A. Vassault, et al. 2005. Muscle-specific loss of apoptosis-inducing factor leads to mitochondrial dysfunction, skeletal muscle atrophy, and dilated cardiomyopathy. *Mol. Cell. Biol.* 25:10261–10272. http://dx.doi.org/10.1128/MCB.25.23.10261-10272.2005

Joza, N., J.A. Pospisilik, E. Hangen, T. Hanada, N. Modjtahedi, J.M. Penninger, and G. Kroemer. 2009. AIF: not just an apoptosis-inducing factor. *Ann. N. Y. Acad. Sci.* 1171:2–11. http://dx.doi.org/10.1111/j.1749-6632.2009.04681.x

Kitamura, D., A. Kudo, S. Schaal, W. Müller, F. Melchers, and K. Rajewsky. 1992. A critical role of lambda 5 protein in B cell development. *Cell*. 69:823–831. http://dx.doi.org/10.1016/0092-8674(92)90293-L

Klein, J.A., C.M. Longo-Guess, M.P. Rossmann, K.L. Seburn, R.E. Hurd, W.N. Frankel, R.T. Bronson, and S.L. Ackerman. 2002. The harlequin mouse mutation downregulates apoptosis-inducing factor. *Nature*. 419:367–374. http://dx.doi.org/10.1038/nature01034

Loeffler, M., E. Daugas, S.A. Susin, N. Zamzami, D. Metivier, A.L. Nieminen, G. Brothers, J.M. Penninger, and G. Kroemer. 2001. Dominant cell death induction by extramitochondrially targeted apoptosis-inducing factor. *FASEB J.* 15:758–767. http://dx.doi.org/10.1096/fj.00-0388com

Maté, M.J., M. Ortiz-Lombardía, B. Boitel, A. Haouz, D. Tello, S.A. Susin, J. Penninger, G. Kroemer, and P.M. Alzari. 2002. The crystal structure of the mouse apoptosis-inducing factor AIF. *Nat. Struct. Biol.* 9:442–446. http://dx.doi.org/10.1038/nsb793

Michie, A.M., and J.C. Zúñiga-Pflücker. 2002. Regulation of thymocyte differentiation: pre-TCR signals and β-selection. *Semin. Immunol.* 14:311–323. http://dx.doi.org/10.1016/S1044-5323(02)00064-7

Moon, E.-Y., Y.H. Han, D.-S. Lee, Y.-M. Han, and D.-Y. Yu. 2004. Reactive oxygen species induced by the deletion of peroxiredoxin II (PrxII) increases the number of thymocytes resulting in the enlargement of PrxII-null thymus. *Eur. J. Immunol.* 34:2119–2128. http://dx.doi.org/10.1002/eji.200424962

Nishimura, H., T. Honjo, and N. Minato. 2000. Facilitation of β selection and modification of positive selection in the thymus of PD-1–deficient mice. *J. Exp. Med.* 191:891–898. http://dx.doi.org/10.1084/jem.191.5.891

Passoni, L., E.S. Hoffman, S. Kim, T. Crompton, W. Pao, M.Q. Dong, M.J. Owen, and A.C. Hayday. 1997. Intrathymic delta selection events in gammadelta cell development. *Immunity*. 7:83–95. http://dx.doi.org/10.1016/S1074-7613(00)80512-9

Pospisilik, J.A., C. Knauf, N. Joza, P. Benit, M. Orthofer, P.D. Cani, I. Ebersberger, T. Nakashima, R. Sarao, G. Neely, et al. 2007. Targeted deletion of AIF decreases mitochondrial oxidative phosphorylation and protects from obesity and diabetes. *Cell*. 131:476–491. http://dx.doi.org/10.1016/j.cell.2007.08.047

Schmitt, T.M., and J.C. Zúñiga-Pflücker. 2002. Induction of T cell development from hematopoietic progenitor cells by delta-like-1 in vitro. *Immunity*. 17:749–756. http://dx.doi.org/10.1016/S1074-7613(02)00474-0

Schmitt, T.M., M. Ciofani, H.T. Petrie, and J.C. Zúñiga-Pflücker. 2004. Maintenance of T cell specification and differentiation requires recurrent notch receptor-ligand interactions. *J. Exp. Med.* 200:469–479. http://dx.doi.org/10.1084/jem.20040394

Schulthess, F.T., S. Katz, A. Ardestani, H. Kawahira, S. Georgia, D. Bosco, A. Bhushan, and K. Maedler. 2009. Deletion of the mitochondrial flavoprotein apoptosis inducing factor (AIF) induces β-cell apoptosis and impairs β-cell mass. *PLoS ONE.* 4:e4394. http://dx.doi.org/10.1371/journal.pone.0004394

Sevrioukova, I.F. 2011. Apoptosis-inducing factor: structure, function, and redox regulation. *Antioxid. Redox Signal.* 14:2545–2579. http://dx.doi.org/10.1089/ars.2010.3445

Srivastava, S., H. Banerjee, A. Chaudhry, A. Khare, A. Sarin, A. George, V. Bal, J.M. Durdik, and S. Rath. 2007. Apoptosis-inducing factor regulates death in peripheral T cells. *J. Immunol.* 179:797–803.

Strasser, A., and P. Bouillet. 2003. The control of apoptosis in lymphocyte selection. *Immunol. Rev.* 193:82–92. http://dx.doi.org/10.1034/j.1600-065X.2003.00036.x

Sun, Z., D. Unutmaz, Y.R. Zou, M.J. Sunshine, A. Pierani, S. Brenner-Morton, R.E. Mebius, and D.R. Littman. 2000. Requirement for RORgamma in thymocyte survival and lymphoid organ development. *Science.* 288:2369–2373. http://dx.doi.org/10.1126/science.288.5475.2369

Taghon, T., M.A. Yui, R. Pant, R.A. Diamond, and E.V. Rothenberg. 2006. Developmental and molecular characterization of emerging β- and gammadelta-selected pre-T cells in the adult mouse thymus. *Immunity.* 24:53–64. http://dx.doi.org/10.1016/j.immuni.2005.11.012

Thompson, L.F., J.G. Vaughn, A.B. Laurent, M.R. Blackburn, and C.J. Van De Wiele. 2003. Mechanisms of apoptosis in developing thymocytes as revealed by adenosine deaminase-deficient fetal thymic organ cultures. *Biochem. Pharmacol.* 66:1595–1599. http://dx.doi.org/10.1016/S0006-2952(03)00530-6

Trigueros, C., K. Hozumi, B. Silva-Santos, L. Bruno, A.C. Hayday, M.J. Owen, and D.J. Pennington. 2003. Pre-TCR signaling regulates IL-7 receptor α expression promoting thymocyte survival at the transition from the double-negative to double-positive stage. *Eur. J. Immunol.* 33:1968–1977. http://dx.doi.org/10.1002/eji.200323831

Urbano, A., U. Lakshmanan, P.H. Choo, J.C. Kwan, P.Y. Ng, K. Guo, S. Dhakshinamoorthy, and A. Porter. 2005. AIF suppresses chemical stress-induced apoptosis and maintains the transformed state of tumor cells. *EMBO J.* 24:2815–2826. http://dx.doi.org/10.1038/sj.emboj.7600746

Vahsen, N., C. Candé, J.-J. Brière, P. Bénit, N. Joza, N. Larochette, P.G. Mastroberardino, M.O. Pequignot, N. Casares, V. Lazar, et al. 2004. AIF deficiency compromises oxidative phosphorylation. *EMBO J.* 23:4679–4689. http://dx.doi.org/10.1038/sj.emboj.7600461

Van De Wiele, C.J., J.G. Vaughn, M.R. Blackburn, C.A. Ledent, M. Jacobson, H. Jiang, and L.F. Thompson. 2002. Adenosine kinase inhibition promotes survival of fetal adenosine deaminase-deficient thymocytes by blocking dATP accumulation. *J. Clin. Invest.* 110:395–402.

Vig, M., S. Srivastava, U. Kandpal, H. Sade, V. Lewis, A. Sarin, A. George, V. Bal, J.M. Durdik, and S. Rath. 2004. Inducible nitric oxide synthase in T cells regulates T cell death and immune memory. *J. Clin. Invest.* 113:1734–1742.

Wiest, D.L., M.A. Berger, and M. Carleton. 1999. Control of early thymocyte development by the pre-T cell receptor complex: A receptor without a ligand? *Semin. Immunol.* 11:251–262. http://dx.doi.org/10.1006/smim.1999.0181

Ye, H., C. Cande, N.C. Stephanou, S. Jiang, S. Gurbuxani, N. Larochette, E. Daugas, C. Garrido, G. Kroemer, and H. Wu. 2002. DNA binding is required for the apoptogenic action of apoptosis inducing factor. *Nat. Struct. Biol.* 9:680–684. http://dx.doi.org/10.1038/nsb836